Postsynthesis of Hexagonally Packed Porous Zirconium Phosphate through a Novel Anion Exchange between Zirconium Oxide Mesophase and Phosphoric Acid

Peng Wu,*,† Yueming Liu,† Minyuan He,† and Masakazu Iwamoto‡

Shanghai Key Laboratory of Green Chemistry and Chemical Processes, Department of Chemistry, East China Normal University, North Zhongshan Road 3663, Shanghai 200062, P. R. China, and Chemical Resources Laboratory, Tokyo Institute of Technology, 4259 Nagatsuta, Midori-ku, Yokohama 226-8503, Japan

Received October 11, 2004. Revised Manuscript Received April 5, 2005

Porous zirconium phosphates having ordered hexagonal pore system and high surface area have been prepared by post-treating surfactant-assisted zirconium oxide mesophase with phosphoric acid solution. The zirconium phosphates with P/Zr atomic ratios of 0.08−1.67 and maintaining totally the hexagonal structure were obtained by varying the phosphoric acid concentration (0.01−1 M), varying the treatment time (0.08−5 h), and repeating the treatment (1−6 times). Zirconium phosphates with P/Zr atomic ratios over 1.0 withstood the calcination up to 873 K and showed the BET specific surface area of 456−547 $m^2\ g^{-1}$. The porous zirconium phosphates were characteristic of micropores with the pore size of 1.30−1.66 nm due to partial condensation of the mesopores during the calcination. The formation mechanism of the hexagonal zirconium phosphates was clarified to be essentially an anion exchange of HPO_4^{2-} ions for SO_4^{2-} ions which mediated the cationic zirconium species and the cationic surfactant headgroups within the as-synthesized zirconium oxide mesophase through electrostatic interactions, together with a reaction between the phosphoric acid and the Zr−OH groups. The anion exchange was confirmed to yield the phosphorus species showing two ^{31}P MAS NMR bands at ca. −3.0 and −9.2 ppm, while the reaction of phosphoric acid with the Zr−OH groups was suggested to form the phosphorus species corresponding to a band at −19.4 ppm.

Introduction

The discovery of a new family of silica or aluminosilicate-based mesoporous materials (M41S), which are formed by a liquid-crystal templating technique and have uniform hexagonal pores of 1.6−10 nm, has opened a new research field in synthesis chemistry.[1] Considerable research interests and intensive studies on this new class of mesoporous materials further developed this technique and led to a cooperative synthesis mechanism for mesoporous materials with the assistance of surfactants. This mechanism is summarized essentially to be a molecular self-assembly of organic templating agents and inorganic oxides.[2] The mesoporous structures are formed through different pathways according to different kinds of interactions between the organic surfactant and the inorganic species. Five pathways, referred to as S^+I^-, S^-I^+, $S^+X^-I^+$ (X = F^-, Cl^-, Br^-, etc.), $S^-M^+I^-$ (M = Na^+, K^+, etc.), and S^0I^0, have been classified based on the physicochemical properties of inorganic species, surfactants, and the synthesis conditions.[3] More recently, a new synthesis route has also been developed using aminosilane or quaternized aminosilane as a co-structure-directing agent to assemble inorganic precursors and anionic surfactants.[4] According to the cooperative mechanism, it should be possible to substitute the silicate with other metal oxides to obtain non-silica mesoporous materials with potential applications as heterogeneous catalysts and sorbents in the processes where high surface area and large pore sizes are necessary for high performance, and also as solid electrolyte devices.

Non-silica mesostructures have been reported for many inorganic metals such as Al,[5] Ti,[6] Ta,[7] Nb,[8] W,[9] Mn,[10] V,[11]

* To whom correspondence should be addressed. Phone: +86-21-6223-2292. Fax: +86-21-6223-2292. E-mail: pwu@chem.ecnu.edu.cn.
† East China Normal University.
‡ Tokyo Institute of Technology.

(1) Kresge, C. T.; Leonowicz, M. E.; Roth, W. J.; Vartuli, J. C.; Beck, J. S. *Nature* **1992**, *359*, 710. Beck, J. S.; Vartuli, J. C.; Roth, W. J. Leonowicz, M. E.; Kresge, C. T.; Schmitt, K. D.; Chu, C. Y.-W.; Olson, D. H.; Sheppard, E. M.; McCullen, S. B.; Higgins, J. B.; Schlenker, J. L. *J. Am. Chem. Soc.* **1992**, *114*, 10834.
(2) Monnier, A.; Schüth, F.; Huo, Q.; Kumar, D.; Margolese, D.; Maxwell, R. S.; Stucky, G. D.; Krishnamurty, M.; Petroff, P. M.; Firouzi, A.; Janicke, M.; Chmelka, B. F. *Science* **1993**, *261*, 1299. Huo, Q.; Margolese, D. I.; Cielsa, U.; Feng, P.; Gier, T. E.; Sieger, P.; Leon, R.; Petroff, P. M.; Schüth, F.; Stucky, G. D. *Nature* **1994**, *368*, 317.
(3) Huo, Q.; Margolese, D. I.; Cielsa, U.; Demuth, D. G.; Feng, P.; Gier, T. E.; Sieger, P.; Firouzi, A.; Chmelka, B. F.; Schüth, F.; Stucky, G. D. *Chem. Mater.* **1994**, *6*, 1176. Tanev, P. T.; Pinnavaia, T. J. *Science* **1995**, *267*, 865.
(4) Che, S.; Liu, Z.; Ohsuna, T.; Sakamoto, K.; Terasaki, O.; Tatsumi, T. *Nature* **2004**, *429*, 281.
(5) Vaudry, F.; Khodabandeh, S.; Davis, M. E. *Chem. Mater.* **1996**, *8*, 1451. Bagshaw, S. A.; Pinnavaia, T. J. *Angew. Chem., Int. Ed. Engl.* **1996**, *35*, 1102.
(6) Antonelli, D. M.; Ying, J. Y. *Angew. Chem., Int. Ed. Eng.* **1995**, *34*, 2014.
(7) Antonelli, D. M.; Ying, J. Y. *Chem. Mater.* **1996**, *8*, 874.
(8) Antonelli, D. M.; Ying, J. Y. *Angew. Chem., Int. Ed. Eng.* **1996**, *35*, 426.
(9) Stein, A.; Fendort, M.; Jarvie, T. P.; Mueller, K. T.; Benesi, A. J.; Mallouk, T. E. *Chem. Mater.* **1995**, *7*, 304.

10.1021/cm0482277 CCC: $30.25
Published on Web 06/29/2005

and Hf[12] and for lacunary Keggin anion $PW_{11}O_{39}$.[13] A common problem, that is, lack of thermal stability, rises for most of these materials when converting them into porous materials by calcination. Exceptions are Al_2O_3 and TiO_2 synthesized with an anionic surfactant and using a phosphate surfactant, respectively. The former can be calcined to remove the surfactant to obtain a mesoporous product having a BET surface area of ca. 700 $m^2\ g^{-1}$, but the pore system is not hexagonally packed for both the as-synthesized and the calcined form.[5] The mesostructure of TiO_2, on the other hand, maintains the hexagonal pore system even after calcination, but it shows a relatively low BET surface area of about 200 $m\ g^{-1}$.[6] Solvent extraction techiniques which are effective in removing the surfactant in the case of MCM-41[14] seem to be unsuitable for most non-silica mesophases, although a successful example is reported for Nb_2O_5 under carefully controlled conditions.[8]

Zirconium mesophases with both random[15] and hexagonal pore structure[16] have been synthesized. The surfactant-assisted zirconium oxide without a regular pore system can be converted by calcination into a porous zirconia with a BET surface area of 329 $m^2\ g^{-1}$,[15] while the zirconium oxide synthesized from the zirconium sulfate source, which possesses a good hexagonal pore system in the as-synthesized form, is totally thermally unstable. Nevertheless, Ciesla et al. reported that a postsynthesis treatment with the phosphoric acid solution would stabilize the structure of this zirconium oxide to stand up to the calcination and obtain a new porous zirconium phosphate with hexagonal structure.[16] The phosphorus agent added directly into the synthesis gel has also been reported to assemble the hexagonal structure for aluminum[17] and vanadium oxides.[18] The formation of the thermally stable mesoporous TiO_2 mentioned above would probably be due to a structure-stabilizing effect of phosphorus because an alkyl phosphate has been used as a template in the synthesis.[6]

The importance of stabilizing effect of phosphorus on non-silica mesoporous oxides has prompted us to investigate the post-treatment of mesoporous zirconium oxide with phosphoric acid, and a unique anionic exchange has been found,[19] which further leads to potential applications of surfactant-assisted zirconium oxide mesophase as selective sorbent in the removal of toxic elements of arsenic and selenium contained in drinking water.[20] Despite these studies, the mechanism for the incorporation of phosphorus is not yet clear, and the coordination states of the phosphorus incorporated in the mesoporous phase has seldom been addressed. In this study, with the purpose of preparing stable porous zirconium phosphate having hexagonal structure and high surface area, we have carried out the phosphoric acid treatment on the as-synthesized zirconium mesophase in detail. The optimum treatment conditions, the mechanism of phosphorus incorporation, and the coordination states of phosphorus have been investigated.

Experimental Section

Synthesis of Hexagonally Mesostructured Zirconium Oxide. Hexagonal zirconium oxide was hydrothermally synthesized from $Zr(SO_4)_2 \cdot 4H_2O$ and hexadecyltrimethylammonium bromide (C_{16}-TMABr) following the procedures reported previously.[16] The gel with a composition of 1.00:0.54:434 $Zr(SO_4)_2$:C_{16}TMABr:H_2O and having a pH of 0.82 was statically heated at 373 K for 48 h. After the crystallization, the white powder product was gathered by filtration, washed thoroughly with deionized water, and dried at 353 K for 12 h. The resultant mesophase of zirconium oxide (abbreviated as Z) was used as a parent sample to prepare zirconium phosphates by the treatment with phosphoric acid solution.

Preparation of Porous Zirconium Phosphate. Porous zirconium phosphate was prepared by treating Z with phosphoric acid solution followed by calcination in air to remove the surfactant. The Z powder was stirred in the H_3PO_4 solution at a solid-to-liquid ratio of 1 g to 20 mL. The H_3PO_4 concentration (0.01−2 M) and the treatment time (0.08−5 h) were varied to investigate their effects on the phosphorus incorporation. The treatment with 0.5 M H_3PO_4 for 2 h was repeated 2−6 times to achieve higher phosphorus incorporation. The acid-treated samples were washed with deionized water and dried at 353 K for 12 h to obtain surfactant-containing zirconium phosphate, ZrP(*n*) where *n* indicates the atomic ratio of P/Zr. The ZrP(*n*) samples were heated at 0.5 K min^{-1} in air to 473−1073 K and calcined at the same temperatures for 6 h to burn off the surfactant.

Characterization Methods. The contents of Zr and P were determined by inductively coupled plasma emission spectrometry (ICP) on a Perkin-Elmer Optima 3000 spectrometer, while those of C, H, and N were measured by the elemental analysis on a Yanagimoto CHN CODER MT-3 analyzer and that of S was determined by ion chromatography on a Dionex DX-500 instrument. X-ray diffraction (XRD) patterns were collected on a MAC Science MXP3 diffractometer using Cu Kα radiation. N_2 adsorption experiment was carried out at 77 K on a Quanta Chrome Autosorb-1 analyzer, while Ar adsorption experiment was carried out at 87 K on a Bel-Japan BELSORP18 analyzer. The specific surface area was calculated according to the standard methods of Brunauer−Emmett−Teller (BET) and Langmuir, while the pore size distribution was calculated by means of the HKSF method[21] from the Ar adsorption isotherm measured at 87 K. Infrared spectra (IR) were recorded on a Bio-Rad FTS-7 spectrometer at a spectral resolution of 2 cm^{-1}. The sample was pressed using the KBr pellet technique into a wafer with 39 mg cm^{-2} thickness. The weight ratio of sample to KBr was 3:100. High-resolution transmission electron micrographs (TEM) were obtained on a JEOL JEM-1200EX II transmission electron microscope operated at 120 kV. The solid-state NMR measurements were performed on a Bruker AC-300 FT-NMR spectrometer equipped with a magic angle spinning (MAS) probe.

(10) Tian, R.; Tong, W.; Wang, Y.; Duan, G.; Krushnan, V. V.; Suob, S. L. *Science* **1997**, *276*, 926.
(11) Luca, V.; MacLachlan, D. J.; Hook, J. M.; Withers, R. *Chem. Mater.* **1995**, *7*, 2220.
(12) Liu, P.; Liu, J.; Sayari, A. *Chem. Commun.* **1997**, 577.
(13) Taguchi, A.; Abe, T.; Iwamoto, M. *Adv. Mater.* **1998**, *10*, 667.
(14) Chen, C.-Y.; Li, X.-H.; Davis, M. E. *Microporous Mater.* **1993**, *2*, 17.
(15) Knowles, J. A.; Hudson, M. J. *J. Chem. Soc., Chem. Commun.* **1995**, 1083.
(16) Ciesla, U.; Schacht, S.; Stucky, G. D.; Unger, K. K.; Schüth, F. *Angew. Chem., Int. Ed. Eng.* **1996**, *35*, 541. Reddy, J. S.; Sayari, A. *Catal. Lett.* **1996**, *38*, 219.
(17) Zhao, D.; Luan, Z.; Kevan, L. *Chem. Commun.* **1997**, 1009. Feng, P.; Xia, Y.; Feng, J.; Bu, X.; Stucky, G. D. *Chem. Commun.* **1997**, 949.
(18) Abe, T.; Taguchi, A.; Iwamoto, M. *Chem. Mater.* **1995**, *7*, 1429.
(19) Wu, P.; Iwamoto, M. *Chem. Lett.* **1998**, 1213.
(20) Iwamoto, M.; Kitagawa, H.; Watanabe, Y. *Chem. Lett.* **2002**, 814. Takada, H.; Watanabe, Y.; Iwamoto, M. *Chem. Lett.* **2004**, 62.
(21) Horváth, G.; Kawazoe, K. *J. Chem. Eng. Jpn.* **1983**, *16*, 470. Saito, A.; Foley, H. C. *AIChE J.* **1991**, *37*, 427. Saito, A.; Foley, H. C. *Microporous Mater.* **1995**, *3*, 531.

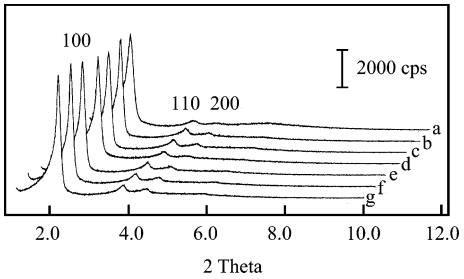

Figure 1. XRD patterns of the parent Z (a) and the ZrP as-synthesized by H_3PO_4 treatment for 0.08 h (b), 0.17 h (c), 0.5 h (d), 1 h (e), 2 h (f), and 5 h (g). The parent Z was treated with 0.5 M H_3PO_4 at a solid-to-liquid ratio of 1 g to 20 mL.

^{31}P MAS NMR spectra were recorded at a resonance frequency of 121.5 MHz and a spinning rate of 5 kHz with phosphoric acid as a chemical shift reference.

Results and Discussion

Preparation of Hexagonal Zirconium Phosphates. The thermal stability of as-synthesized zirconium oxide mesophase has been investigated by raising the calcination temperature stepwise from 373 to 873 K. The hexagonal structure of the parent Z was totally collapsed after calcination in air at 573 K for 6 h as indicated by XRD (not shown), while a large amount of surfactant still remained in the bulk. Therefore, the structure-stabilizing modifications are necessary in order to enhance its thermal stability and to convert it finally into a porous material. The modification method with H_3PO_4 treatment was adopted here to stabilize the structure of zirconium oxide.

The H_3PO_4 treatment was carried out on the as-synthesized Z to investigate the optimum conditions for introducing phosphorus into the mesophase. The effect of treatment time on the P incorporation was first investigated using 0.5 M H_3PO_4. The starting pH of the solution was 1.13 and was not further adjusted. After the treatment for 0.08−5 h, the pH value dropped to 0.88−0.95 and the sample weight of the solid product was increased by 0.5−4.5 wt %. The latter phenomenon is totally different from the HCl treatment of as-synthesized MCM-41,[14] where the sample always decreases its weight due to the removal of the surfactant cations. This suggests that it is difficult for the phosphorus incorporation to be a result of the exchange of phosphate ions with the heavier surfactant species. The results concerning the surfactant removal will be given in a later section. Figure 1 shows the XRD patterns before and after the acid treatment for a different period of time. The pattern Z showed three characteristic diffractions corresponding to *d* spacings of 4.06, 2.36, and 2.03 nm (Figure 1a), which are similar to those reported previously and are indexed as (100), (110), and (200) of a hexagonal structure.[16] After the acid treatment, the hexagonal structure was maintained totally and the pore array even became more orderly (Figure 1b−g). A slight increase in the intensity of the (100) diffraction was observed after the acid treatment (Figure 2). On the other hand, the amount of phosphorus incorporated into the solid, expressed as the atomic ratio of P/Zr, increased rapidly at the initial stage of the treatment and approached a saturated value after 2 h. The phosphorus incorporation was achieved by ca. 80%

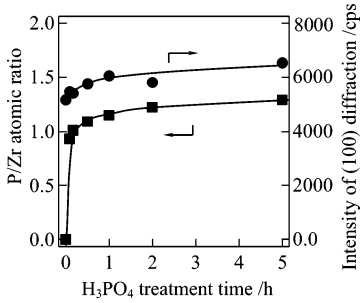

Figure 2. Effect of H_3PO_4 treatment time on the P/Zr atomic ratio and the (100) diffraction intensity of as-synthesized ZrP. For H_3PO_4 treatment conditions, see Figure 1.

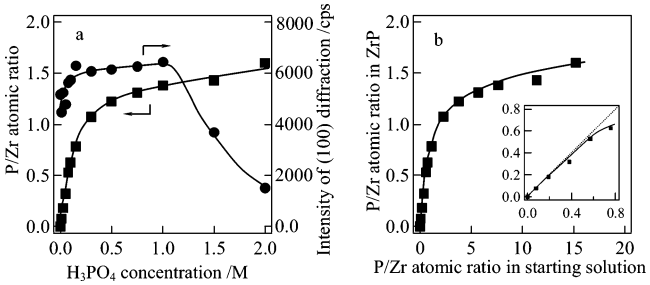

Figure 3. Effect of H_3PO_4 concentration on the P/Zr atomic ratio and the intensity of the (100) diffraction (a) and the P/Zr atomic ratio in the ZrP as a function of the P/Zr atomic ratio in the starting solution (b). The inset in b shows the change at low P/Zr ratio. The parent Z was treated with 0.01−2 M H_3PO_4 for 2 h at a solid-to-solution ratio of 1 g to 20 mL.

within the first 0.08 h, indicating a very rapid interaction between the as-synthesized zirconium oxide mesophase and the H_3PO_4 solution.

The effect of H_3PO_4 concentration on the phosphorus incorporation was investigated when the treatment time was fixed at 2 h. The starting pH of the solution was 2.15−0.39 for the H_3PO_4 solution of 0.01−2 M. Again a decrease in the pH value and an increase in the weight were observed after the treatment. The XRD measurements verified that the ZrP products obtained in the H_3PO_4 solution of 0.01−1 M exhibited good hexagonal structure, whereas those prepared in the H_3PO_4 solution with higher concentrations showed lower intensity of the (100) diffraction (Figure 3a). Especially, the ZrP sample prepared with 2 M H_3PO_4 lost the (110) and (200) diffractions completely and showed only a very broad (100) XRD diffraction. Therefore, to prepare the ZrP with a regular hexagonal structure, it is necessary to use the H_3PO_4 solution with concentrations below 1 M. The P/Zr atomic ratio in the ZrP products shown in Figure 3a as a function of the H_3PO_4 concentration increased greatly in the region of 0.01−0.5 M and slightly increased in the region 0.5−2 M. To know how efficiently the phosphorus was incorporated into the solid, the P/Zr ratio in the ZrP product is plotted against that in the starting solution in Figure 3b. Nearly all of the phosphorus was incorporated into the matrix of zirconium oxide when the starting P/Zr ratio was lower than 0.8, while the amount of phosphorus gradually became excessive in the solution over the P/Zr ratio of 0.8.

The ZrP with high P/Zr ratio can be prepared by using concentrated H_3PO_4 solution; however, as evidenced by XRD (Figure 3a), it is difficult for the hexagonal structure to withstand the treatment by the H_3PO_4 solution more acidic than 1 M. To investigate the limitation of the phosphorus

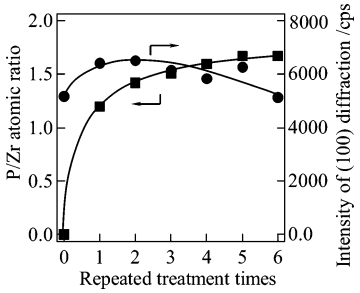

Figure 4. Effect of repeated H_3PO_4 treatment on the P/Zr atomic ratio and the intensity of the (100) diffraction. For each treatment, the parent Z or the ZrP was treated with 0.5 M H_3PO_4 for 2 h at a solid-to-solution ratio of 1 g to 20 mL.

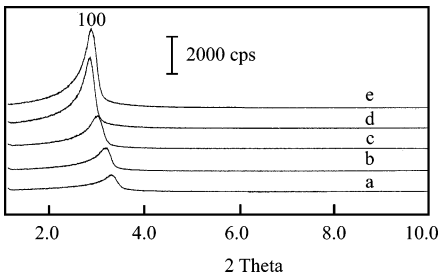

Figure 5. XRD patterns of the calcined ZrP samples with the P/Zr atomic ratio of 0.78 (a), 1.07 (b), 1.22 (c), 1.50 (d), and 1.67 (e). The calcination was carried out in air at 723 K for 6 h.

incorporation, the parent Z was treated repeatedly using 0.5 M H_3PO_4 solution for 2 h. The first treatment made the P/Zr ratio of the ZrP increase greatly, and the P/Zr ratio was further increased little by little by repeating the treatment, reaching a maximum of 1.67 after five treatments (Figure 4). The sixth treatment did not lead to more phosphorus incorporation but caused a slight decrease in the intensity of the (100) diffraction. Thus, ZrP maintaining a highly ordered hexagonal structure could be prepared to have a maximum P/Zr ratio of ca. 1.7 by the present postsynthesis method, although the conventional crystalline zirconium phosphates such as α-, γ-, and ω-ZrP have the formulas of ZrP_2O_7 or $Zr(HPO_4)_2$.[21] As a result, we have succeeded in preparing the hexagonal zirconium phosphates with various P/Zr ratios of 0.08−1.67 by varying the treatment time and the H_3PO_4 concentration, and also by repeating the treatment.

Porous Properties of Hexagonal Zirconium Phosphates. The ZrP samples thus postsynthesized were calcined in air to remove the surfactant to obtain porous materials. ZrP with a Zr/P ratio of 1.50 was calcined in air at 473−1073 K for 6 h to investigate its thermal stability upon calcination. The XRD patterns verified that its hexagonal structure was maintained up to 873 K. Since the surfactant was removed by ca. 100% after calcination at 723 K for 6 h, this calcination condition was used to obtain the porous ZrP. The calcined samples showed only one peak due to the (100) diffraction in the XRD patterns, but no longer well-resolved (110) and (200) diffractions (Figure 5). The intensity of the (100) diffraction increased with increasing P/Zr ratio. Its peak position shifted to higher 2θ region to give smaller *d* spacings when compared with that of the as-synthesized Z, which indicates condensation still occurred during calcination even after stabilizing the structure with the H_3PO_4 treatment. The *d* spacing of the (100) diffraction increased from 2.67 to 3.15 nm for the ZrP when the P/Zr ratio varied from 0.78 to 1.67.

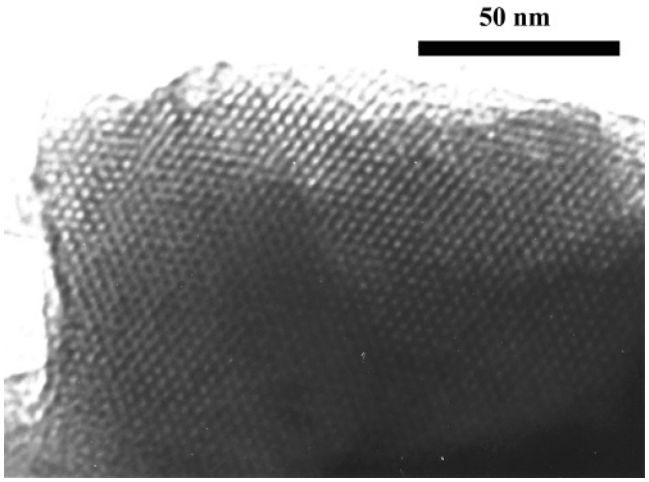

Figure 6. Transmission electron micrograph of the calcined ZrP(1.67).

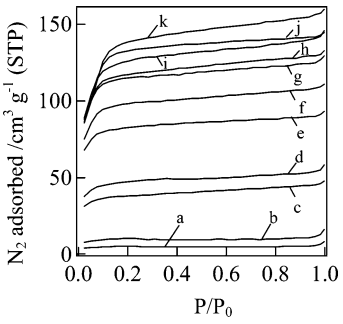

Figure 7. N_2 adsorption isotherms at 77 K for the calcined Z (a) and the calcined ZrP with the P/Zr ratio of 0.32 (b), 0.53 (c), 0.62 (d), 0.78 (e), 1.01 (f), 1.07 (g), 1.22 (h), 1.50 (i), 1.59 (j), and 1.67 (k).

Therefore, the lower the amount of phosphorus incorporated, the more serious the condensation. The transmission electron micrograph was consistent with the XRD measurements to confirm the presence of hexagonally packed pores within the ZrP after removal of the surfactant (Figure 6). The *d* spacing of ZrP(1.67), ca. 2.9 nm, determined from the micrograph was somewhat smaller than the value of 3.15 nm from XRD measurements. Condensation was observed when the sample particles were irradiated by the electron beam during the TEM measurements, which probably accounts for the difference in *d* value observed above.

N_2 adsorption measurements showed that the porous properties of ZrP greatly depended on the P/Zr ratio. The volume of N_2 adsorbed increased with increasing P/Zr ratio from 0 to 1.67 (Figure 7). The position of the steep increase in adsorbed volume also changed with the P/Zr ratio; that is, the increase was almost not observed for the ZrP with the P/Zr ratio lower than 0.78 (Figure 7a−e), while a slight increase around a relative pressure of 0.15 was observed for ZrP with the P/Zr ratio over 1.01 (Figure 7f−k). However, the steep increase was not as obvious as the representative mesoporous material, MCM-41. This can be taken as evidence for the presence of micropores in these ZrP materials. Considering this particularity, we evaluate here the specific surface area of hexagonal ZrP using both the BET and the Langmuir methods. Especially, the BET surface area was calculated using the adsorption data at the relative pressure lower than 0.1 to reduce the overestimation due to the condensation of N_2 adsorbing from micropores to

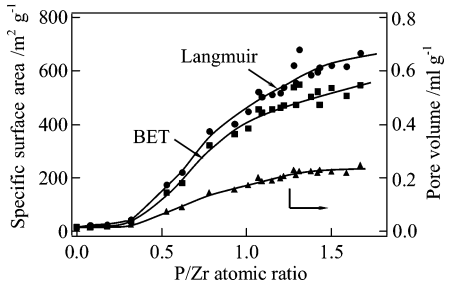

Figure 8. BET surface area, Langmuir surface area, and pore volume as a function of P/Zr ratio in the calcined ZrP samples.

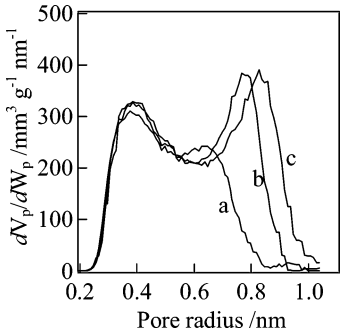

Figure 9. Pore size distributions of the calcined ZrP with the P/Zr atomic ratio of 0.99 (a), 1.61 (b), and 1.67 (c). The distributions were determined by the HKSF method using Ar adsorption isotherm at 87 K.

mesopores. The specific area (both BET and Langmuir) and the pore volume increased with increasing P/Zr ratio and approached maximums when the P/Zr ratio was over 1.0 (Figure 8). The region where they increased sharply was at the P/Zr ratio of 0.6−0.8, the reason about which will be discussed in a later section. The BET surface area of 456−547 $m^2\ g^{-1}$ observed for the ZrP samples with the P/Zr ratio of 1.07−1.67 may be among the highest values obtained with zirconia, sulfated zirconia, and zirconium phosphates so far to the best of our knowledge.

Since the N_2 adsorption measurements with the BJH method do not give reliable pore size for the present ZrP samples containing micropores,[16] the Ar adsorption measurements at 87 K were employed to calculate the pore distribution with the HKSF method.[21] The magnetic susceptibility of wall atom (χ_E) was set at -1.9×10^{-29} cm^3, which has been applied successfully for the calculation of $AlPO_4$-5, VPI-5, and heteropolyacids.[21,23] The pore distributions thus obtained are shown in Figure 9. Since the peaks around 0.38 nm could be due to the erroneous calculation of the multilayer adsorption of Ar molecules on the wall, we would not discuss them further. The pore radius was 0.65, 0.77, and 0.83 nm for ZrP(0.99), ZrP(1.61), and ZrP(1.67), respectively, that is, slightly increased with increasing P/Zr ratio, which supports the above XRD data to verify that incorporating more phosphorus into the zirconium oxide would prevent more effectively the pores from condensing upon calcination. The relative broad distributions show again that the hexagonal pore arrangement of ZrP is not as ordered as conventional MCM-41.

(22) Segawa, K.; Kurusu, Y.; Nakajima, Y.; Kinoshita, M. *J. Catal.* **1985**, *94*, 491.
(23) Yamada, T.; Johkan, K.; Okuhara, T. *Microporous Mesoporous Mater.* **1998**, *26*, 109.

Table 1. Elemental Analysis Data

sample	H_3PO_4 treatment[a] concn (M)	repeated times	P (mmol g^{-1})	C/N ratio	C_{16}TMA (mmol g^{-1})	Br (mmol g^{-1})	S (mmol g^{-1})
Z	parent		0	18.4	1.43	0.05	2.35
ZrP(0.08)	0.01	1	0.19	17.2	1.35	0.01	2.09
ZrP(0.32)	0.05	1	0.83	19.0	1.30	0.00	1.49
ZrP(0.62)	0.10	1	1.71	18.7	1.27	0.00	0.81
ZrP(1.07)	0.30	1	2.66	17.2	1.26	0.00	0.40
ZrP(1.22)	0.50	1	2.95	18.2	1.27	0.00	0.19
ZrP(1.50)	0.50	3	3.58	21.2	1.21	0.00	0.02
ZrP(1.67)	0.50	5	3.65	17.1	1.18	0.00	0.05

[a] The treatment was carried out at a solid-to-liquid ratio of 1 g to 20 mL for 2 h.

Phosphorus Incorporation Mechanisms. The treatment of surfactant-containing zirconium oxide with H_3PO_4 solution leads to hexagonal ZrP composites which can be converted into porous materials with high specific area by calcination. We try to clarify here the incorporation mechanism of phosphorus and the reason the structure can be stabilized as a result of phosphorus incorporation. It has been reported for MCM-41 that the surfactant is extracted readily from the as-synthesized composite by HCl.[14] To investigate whether the phosphorus incorporation was related to the release of surfactant during the H_3PO_4 treatment, the amount of surfactant was determined by elemental analysis for all the samples. Table 1 lists the data of several representatives from a series of samples prepared under similar conditions. The C/N atomic ratio of the as-synthesized Z was very near the theoretical value of 19 for C_{16}TMA cation. The Z contained only a trace amount of Br which originated from the C_{16}-TMABr molecules not washed away thoroughly with water. This part of Br was completely removed by the H_3PO_4 treatment. These results indicate that nearly all the surfactant was in the cationic state constructing the structure of the mesophase. A slight decrease in the amount of C_{16}TMA was observed after the H_3PO_4 treatment, but ZrP(1.67) with the maximum phosphorus content still contained 83% of C_{16}-MTA as compared to the parent Z. Since the amount of the surfactant released during the treatment was much smaller than that of phosphorus incorporated, the phosphorus incorporation thus is hardly ascribed to the reaction or ion exchange between H_3PO_4 and the surfactant species. The fact that, as mentioned earlier, the sample weight increased after the treatment also supports this conclusion. Thus, other incorporation routes should be considered.

It is generally agreed that the synthesis of mesoporous materials with a surfactant template takes place according to a cooperative mechanism which always involves a charge interaction between the constituent elements and the surfactant molecules.[2,3] The present hexagonal zirconium oxide was synthesized from a strongly acidic zirconium source, $Zr(SO_4)_2$, and a cationic surfactant of C_{16}TMABr. $Zr(SO_4)_2$ may react with the positively charged surfactant headgroups to form a SO_4^{2-}-mediated unit like $Zr-SO_4-C_{16}$TMA composite which is subsequently self-assembled into a hexagonal structure through a so-called $S^+X^-I^+$ pathway. Those mediating SO_4^{2-} ions left within the as-synthesized mesophase may correspond to the phosphorus incorporation. The amount of sulfur was thus determined also by the elemental analysis. It is obvious that a progressive incorpora-

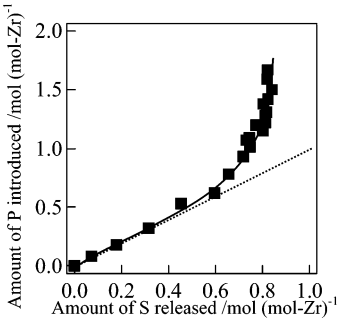

Figure 10. Relationship between the amount of phosphorus incorporated and that of sulfur released. The dotted line shows the P:S ratio of 1:1.

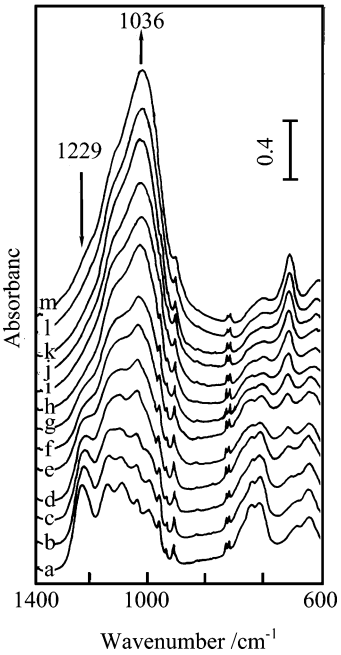

Figure 11. IR spectra of the parent Z (a) and the as-synthesized ZrP with the P/Zr atomic ratio of 0.08 (b), 0.18 (c), 0.32 (d), 0.53 (e), 0.62 (f), 0.78 (g), 1.07 (h), 1.22 (i), 1.38 (j), 1.42 (k), 1.59 (l), and 1.67 (m).

tion of phosphorus made the sulfur be released gradually (Table 1). The amount of phosphorus incorporated as a function of the amount of sulfur released is shown in Figure 10. There is good correlation between these two variables. Especially, when the amount of phosphorus incorporated was below the P/Zr ratio of 0.8, releasing every sulfur atom led to incorporating a phosphorus atom. On the basis of this result, we suggest that an anion exchange between the phosphoric acid and the sulfate ions contributes greatly to the incorporation of phosphorus into the zirconium mesophase.

IR measurements were carried out to give more essential evidence for the anion exchange proposed above (Figure 11). The parent Z showed the strongest band at 1229 cm^{-1} together with several overlapped ones in the 1300−1000 cm^{-1} region (Figure 11a). The multiplicity of the bands in this region is generally assigned to the S−O stretching vibrations of surface sulfates in the case of sulfated zirconia.[24] The sharp but very weak bands at 1000−900 cm^{-1} and at

(24) Morterra, C.; Cerrato, G.; Pinna, F.; Signoretto, M. *J. Phys. Chem.* **1994**, *98*, 12373. Morterra, C.; Bolis, V.; Cerrato, G.; Magnacca, G. *Surf. Sci.* **1994**, *307*−*309*, 1206. Platero, E. E.; Mentruit, P.; Arean, C. O.; Zecchina, A. *J. Catal.* **1996**, *162*, 268.

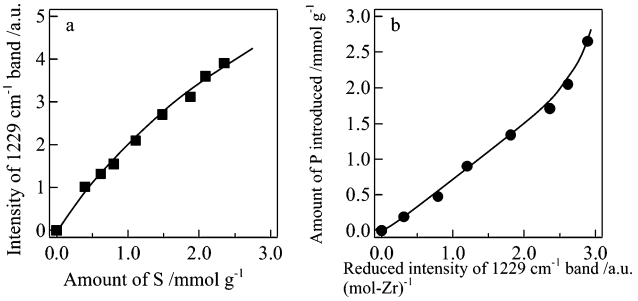

Figure 12. Intensity of the 1229 cm^{-1} S−O band as a function of the sulfur amount (a) and the amount of phosphorus incorporated as a function of the reduced intensity of the 1229 cm^{-1} S−O band (b).

800−700 cm^{-1} were consistent with those observed for C_{16}-TMABr. These surfactant-related bands were not affected by the H_3PO_4 treatment, while the 1229 cm^{-1} band decreased in the intensity gradually and finally disappeared (Figure 11b−m). Simultaneously, a new broad band with the top position at 1036 cm^{-1} was developed. This band, probably containing several overlapped bands, increased in intensity with increasing P/Zr ratio, and it is attributed to the P−O stretching and bending vibrations following the previous assignments for the crystalline zirconium phosphate.[22] For more quantitative considerations, the absorbance of the 1229 cm^{-1} band was measured. The intensity of the 1229 cm^{-1} band was nearly proportional to the sulfur amount remaining within the sample (Figure 12a). The amount of phosphorus incorporated, on the other hand, proportionally increased with the reduced intensity of the band (Figure 12b). These results are in agreement with that of Figure 10 to confirm the anion exchange of phosphate ions for sulfate ions during the H_3PO_4 treatment. The H_3PO_4 acid dissociates in the aqueous solution at least into three kinds of anions, that is, PO_4^{3-}, HPO_4^{2-}, and $H_2PO_4^{-}$, whose relative concentrations depend on the pH. Considering that the sulfur is released out as SO_4^{2-} ions and the conventional zirconium phosphates are formed as $Zr(HPO_4)_2$,[22] we prefer to propose the anion exchange proceeds dominantly through the HPO_4^{2-} ions for SO_4^{2-} ions as shown in Scheme 1.

Scheme 1

$$\text{Zr-SO}_4\text{-C}_{16}\text{TMA} + \text{H}_3\text{PO}_4 \longrightarrow \text{Zr-HPO}_4\text{-C}_{16}\text{TMA} + \text{H}_2\text{SO}_4$$

The SO_4^{2-} ions released from the solid composite would form H_2SO_4 in the acidic solution. Since H_2SO_4 has a much larger dissociation constant than H_3PO_4, the pH of the solution decreased after the treatment as mentioned earlier.

Figure 10 shows us that the phosphorus incorporation still proceeded when the P/Zr ratio was over 0.8, where the sulfur was already lowered to a minimum level. Therefore, other sites into which the phosphorus can be incorporated presumably exist within the as-synthesized composite. Further reaction of phosphoric acid with HPO_4^{2-} ions formerly incorporated through the anion exchange for SO_4^{2-} ions to yield polyphosphoric species may correspond to one possible reason for above phenomenon. If this reaction really occurred, the P−O−P vibration bands would be observed at 980 and 750 cm^{-1}.[22] However, no such bands were observed for the ZrP samples with the P/ Zr ratio higher than 0.8 in their spectra (Figure 11h−m). The present zirconium me-

sophase was synthesized from a strongly acidic gel with pH < 1. The aqueous chemistry of zirconium indicates that zirconium ions are easily protonated to form species such as polymeric $[Zr(OH)_2SO_4(H_2O)]$ units[25] or tetranuclear $[Zr_4(OH)_8(H_2O)_{16}]^{8+}$ ions.[26] After hydrothermal crystallization, a part of the hydroxyl groups attached to zirconium ions may condense whereas the other part of them still remain in the hexagonal structure formed. Therefore, the phosphate ions probably would react with those remaining Zr−OH groups as suggested by Ciesla et al.[16] Scheme 2 gives the simplest model to describe this reaction corresponding to another kind of phosphorus incorporation.

Scheme 2

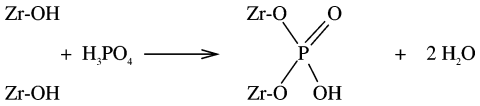

The feature of Figure 10 indicates that the phosphorus incorporation through anion exchange proceeds more rapidly than that through the reaction of H_3PO_4 with Zr−OH groups. However, the phosphate ions incorporated according to Scheme 2 would cross-link the zirconium ions to form a regional ZrP matrix within the structure. This is expected to stabilize the hexagonal structure through preventing the condensation of ZrO_2. On the other hand, those phosphate ions formed through Scheme 1 cannot stabilize the structure effectively because they are coordinated in an isolated manner to the Zr ions on the inside surface of the mesopores. This is the reason the high specific area and large pore volume were observed for the ZrP samples only when their P/Zr ratios were over 0.8 (Figure 8), that is, in the region where more structure stabilizing phosphate ions in Scheme 2 were incorporated.

Coordination States of Phosphate Ions. ^{31}P MAS NMR spectra were measured to characterize the phosphorus microenvironment in the hexagonal ZrP. Figure 13 shows the spectra of ZrP samples without calcination. Incorporating a small amount of phosphorus developed a band at −9.2 ppm which was not observed for the parent Z (Figure 13a,b). When the P/Zr ratio increased, the intensity of the −9.2 ppm band increased, and a new band simultaneously appeared around −3.0 ppm (Figure 13c−h). Another new shoulder band was developed at higher magnetic field compared to the −9.2 ppm band following further incorporation of phosphorus into the mesophase (Figure 13i−p), and this shoulder finally became the most intensive band at −19.4 ppm for ZrP(1.67). Therefore, hexagonal ZrP at least has three kinds of phosphorus environments which correspond to the different environments or coordination states of the phosphate groups. The relative content of each kind of phosphorus closely depends on the phosphorus incorporation level.

To obtain more quantitative insight into these three bands, the spectra were deconvoluted by computer simulation

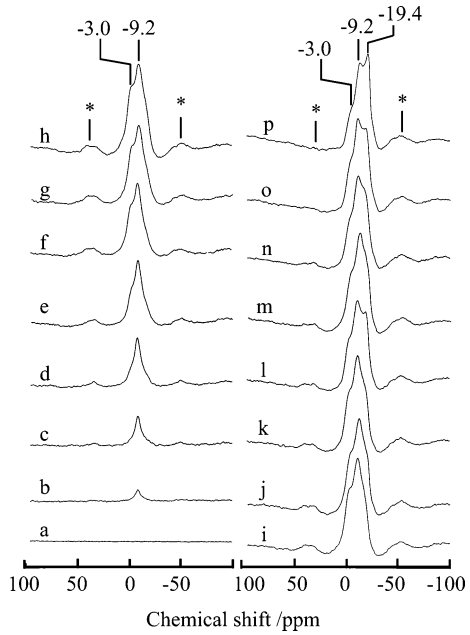

Figure 13. ^{31}P MAS NMR spectra of the parent Z (a) and the ZrP with the P/Zr atomic ratio of 0.08 (b), 0.18 (c), 0.32 (d), 0.53 (e), 0.62 (f), 0.78 (g), 1.07 (h), 1.22 (i), 1.28(j), 1.31 (k), 1.38 (l), 1.42 (m), 1.50 (n), 1.59 (o), and 1.67(p).

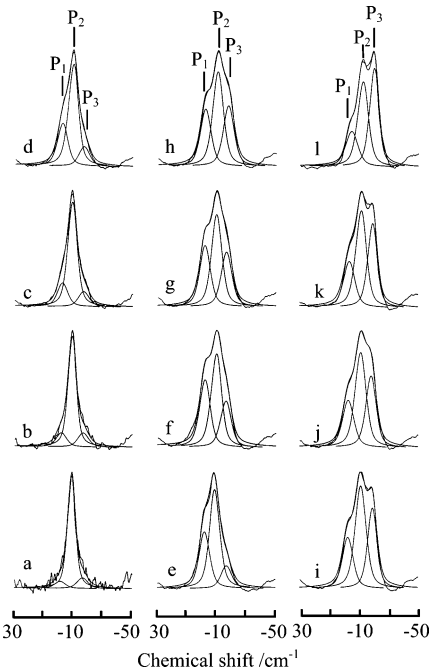

Figure 14. Simulated ^{31}P MAS NMR spectra of the ZrP with the P/Zr atomic ratio of 0.08 (a), 0.18 (b), 0.32 (c), 0.53 (d), 0.62 (e), 1.07 (f), 1.22 (g), 1.31 (h), 1.38 (i), 1.50 (j), 1.59 (k), and 1.67(l).

(Figure 14). The width was nearly the same (1.05 ± 0.1 kHz) for the three bands, while the band position slightly shifted toward higher magnetic field with increasing P/Zr ratio in the regions of −1.3 to −3.6 ppm, −9.0 to −11.5 ppm, and −16.6 to −19.7 ppm, respectively. We would mark three bands as P_1, P_2, and P_3 to simplify the expression here. The band area normalized to the same sample weight is shown in Figure 15a as a function of the phosphorus amount. The total area of the bands was proportional to the phosphorus amount in the region 0−3.2 mmol g^{-1}, but was almost the same in the region of larger phosphorus amount. This is probably due to the existence of "NMR-invisible" phosphorus

(25) Livage, J.; Henry, M.; Sanchez, C. *Prog. Solid State Chem.* **1988**, *18*, 259.
(26) Devia, H.; Sykes, A. G. *Inorg. Chem.* **1981**, *20*, 910. Thompson, R. C. *Inorg. Chem.* **1985**, *25*, 3542.

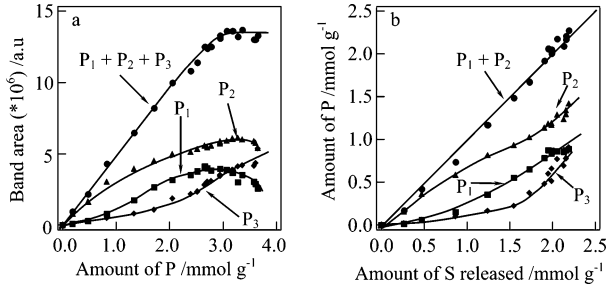

Figure 15. Band area as a function of the phosphorus amount (a) and the phosphorus amount of individual band as a function of the amount of sulfur released (b).

species within the ZrP samples having the phosphorus amount over 3.2 mmol g^{-1}. Although the NMR-invisible phosphorus species have seldom been reported in the literature, the NMR-invisible aluminum species are very common for zeolites when they exist in a distorted coordination state or lose the symmetry.[27] The relationship between the individual band area and the phosphorus amount revealed to us that the area of the P_3 band increased monotonically with increasing the phosphorus amount, while those of P_1 and P_2 increased first and then decreased slightly when the phosphorus amount was over 3.2 mmol g^{-1}. Thus, the NMR-invisible phosphorus species are presumably from the P_1 and P_2 species. Since these two species formed more rapidly than the P_3 species as depicted in Figure 13, they may interact with the phosphorus species formed afterward during the repeated H_3PO_4 treatment to alter the environment partially into NMR-invisible states.

The behaviors of P_1 and P_2 different from that of P_3 suggest that they were formed through the different routes, for example, according to Schemes 1 and 2, respectively. To clarify this issue, each phosphorus species was quantified based on the band area and the total phosphorus amount determined by ^{31}P MAS NMR and ICP, respectively. The phosphorus amount thus obtained is plotted against the amount of sulfur released in Figure 15b for the ZrP samples which showed the proportional relationship between the total band area and the phosphorus amount in Figure 15a. Both the amount of P_1 and that of P_2 were nearly proportional to the amount of sulfur released, while the P_3 amount showed again a different behavior, that is, almost varied little when the amount of sulfur released was high at low scale levels but increased drastically when the sulfur released was low at high scale levels. This result suggests that the P_1 and P_2 species may be assigned to the phosphate ions formed through the anion exchange for the sulfate ions (Scheme 1) and that the P_3 species is due to those phosphate ions formed through the reaction with Zr−OH groups (Scheme 2). In fact, the sum amount of P_1 and P_2 was proportional to the amount of sulfur released at a slope of unit (Figure 15b).

The assignment of the P_3 band to the phosphorus species in Scheme 2 is also supported by the fact that its chemical shift of ca. −19 ppm is similar to that reported for α-ZrP and ZrP gel in which the phosphate ions are directly bonded to the Zr ions.[28] On the other hand, the phosphorus species bonded to zirconium species and organic groups simultaneously in zirconium phosphates of $Zr(O_3PR)_2$ generally chemically shift toward lower magnetic fields.[29] As viewed to this point, it is also reasonable to assign the P_1 and P_2 band to the phosphorus species mediating the zirconium ions and the cationic surfactant groups as shown in Scheme 1 since they showed the chemical shifts at lower magnetic field when compared to the P_3 band. However, further study is needed to make clear why the phosphate ions in Scheme 1 showed two kinds of microenvironments giving the P_1 and P_2 bands.

Conclusions

Porous zirconium phosphates with hexagonal structure have been postsynthesized through an anion exchange of HPO_4^{2-} ions for SO_4^{2-} ions which are contained within the surfactant-assisted zirconium oxide mesophase, together with a reaction of phosphoric acid with uncondensed Zr−OH groups. The novel anion exchange revealed during the phosphoric acid treatment suggests that as-synthesized zirconium oxide mesophase has potential application as a sorbent for removal of the anions contained in the pollution of the environment. On the other hand, the hexagonal zirconium phosphates possessing surface area as high as 456−547 m^2 g^{-1} are expected to be applied as more effective catalysts for those reactions catalyzed by the conventional zirconium phosphates. Furthermore, the present porous zirconium phosphates still contain a small amount of sulfur even after the anion exchange and calcination. This part of sulfur in the form of sulfate groups would develop on the surface of the zirconium phosphates the superacid sites such as those on sulfated zirconia, which makes porous zirconium phosphates important acidic catalysts for special reactions.

Acknowledgment. We thank for financial support the National Natural Science Foundation of China (Grants No. 20473027 and 20233030) and Science and Technology Commission of Shanghai Municipality (03DJ14005).

CM0482277

(27) Shertukde, P. V.; Hall, W. K.; Dereoppe, J.-M.; Marcelin, G. *J. Catal.* **1993**, *139*, 468. Wu. P.; Komatsu, T.; Yashima, T. *J. Chem. Soc., Faraday Trans.* **1996**, *92*, 861.

(28) Segawa, K.; Nakajima, Y.; Nakata, S.; Asaoka, S.; Takahashi, H. *J. Catal.* **1986**, *101*, 81.

(29) Segawa, K.; Sugiyama, A.; Kurasu, Y. *Stud. Surf. Sci. Catal.* **1991**, *60*, 73. Segawa, K.; Kiharar, N.; Yamamoto, H.; *J. Mol. Catal.* **1992**, *74*, 21.